



EISSN: 2788-9920  
NTU Journal for Renewable Energy  
Available online at:  
<https://journals.ntu.edu.iq/index.php/NTU-JRE>



## Comparison of Heat Sinks with Different Perforations Numbers

Rana A. J. AL-Luhaibi <sup>1</sup>, Ibrahim T. Nazzal<sup>2</sup>

<sup>1,2</sup>Mechanical Department/ Engineering College /Tikrit University/ Tikrit, Iraq.

### Article Informations

Received: 10 – 09 - 2023  
Accepted: 28 – 09 - 2023  
Published: 02 – 10 - 2023

### Corresponding Author:

Rana A. J. AL-Luhaibi

### Email:

[rana.a.jasim43787@st.tu.edu.iq](mailto:rana.a.jasim43787@st.tu.edu.iq)

### Key words:

Forced convection, heat sink,  
Perforated heat sink,  
perforation diameter.

### ABSTRACT

In this paper, the influence of perforation number  $N_p$  is experimentally studied (or in the other word, the effect of perforation space  $P_s$  on the heat sink performance). Three types of rectangular heat sinks were investigated; two types have been perforated by lateral holes (4 mm the hole diameter) distributed on two rows in the fin. First one has 12 holes in a fin (its  $P_s$  is 14.3mm) called (PHS-12p). Second heat sink has 8 holes in a single fin (its  $P_s$  is 20mm) called (PHS-8p). These two perforated types compared with the third heat sink, which has no perforation (solid heat sink). The comparison was investigated, presented and discussed. The experiment was conducted by forced convection device. The obtained results showed that dissipated heat, Nusslet number, and convective heat transfer coefficient were increased by using perforations compared with non-perforated heat sink. The use of more perforations has a positive effect on heat dissipation. The enhancement in heat transfer was 6.57% for PHS-12P, while PHS\_8P improved by 1.75% only at  $Re$  20000. Moreover, the heat sink weight decreases with the use perforated heat sink compared with the solid heat sink.



© THIS IS AN OPEN ACCESS ARTICLE UNDER THE CC BY LICENSE: <https://creativecommons.org/licenses/by/4.0/>

## 1. Introduction

Nowadays, a great development of electronic devices is taking place, resulting in an increase in the amount of heat they generate. Consequently, effectively dissipating this heat has become the primary challenge in enhancing the cooling of such devices. One commonly utilized method for heat dissipation is the implementation of plate fin heat sinks due to their manufacturing simplicity. The optimization of rectangular plate fins' performance has been extensively explored by numerous researchers over the past few decades. Several studies have also investigated methods to enhance heat transfer in heat sinks by modifying the fin geometry [1], introducing vortex generation to the fins [2], and incorporating ribs into the heat sink passages [3][4]. Furthermore, the impact of using perforated fins has been examined by several researchers. For instance, Sara et al. [5] conducted an experimental investigation on the pressure drop and heat transfer across perforated flat plates, revealing that the use of perforated fins resulted in increased heat dissipation compared to solid flat plates. Shaeri et al. [6](2009) conducted a numerical investigation on the fluid flow and convective heat transfer of rectangular perforated fins with square holes positioned on the side of the fins. Their findings revealed that the new perforated fins exhibited higher overall heat transfer rates and significantly reduced weight compared to solid fins. Venkataraj and Siddikh [7](2016) employed numerical analysis to assess the enhancement in convection heat transfer achieved by an array of fins. They examined various types of perforations, including circular, elliptical, square, and triangular, to evaluate their performance and material mass. Their results demonstrated that the fin with a circular perforated array exhibited superior performance compared to the other types studied. Sonawane and Palande [8](2016) investigated the potential for improving heat transfer in fin heat sinks through different perforation designs. Perforated pin-fin heat sinks were found to offer higher heat transmission rates compared to solid pin-fin heat sinks. Shaeri et al. [9](2017) conducted an experimental investigation to compare the hydraulic and thermal performance of laterally perforated-finned heat sinks. They utilized three different sizes of square cross-sectional perforations evenly distributed along the heat sinks' length. Their findings indicated that the perforated

fins exhibited higher heat dissipation compared to unperforated fins. Chingulpitak et al. [10](2019) presented the thermal performance of laterally perforated plate-fin heat sinks with varying numbers and diameters of circular perforations. The study recommended considering the thermal performance factor, which incorporates the Nusselt number and friction factor, to determine appropriate design parameters. Compared to solid heat sinks, the perforated heat sinks demonstrated a 10.6% improvement in thermal performance and a 28% reduction in mass. Huang et al. [11](2021) investigated the thermal performance of pin-fin heat sinks with perforations and splitters. Their study revealed a significant improvement in thermal performance attributed to the presence of perforations and splitters.

In summary, the addition of holes in the fins of plate-fin heat sinks has been introduced as a means to enhance their thermal performance. The types, numbers, and sizes of perforations are considered influential factors in improving heat sink performance. Despite ongoing research on the effects of perforated fins on heat sink performance, further exploration is still warranted. This paper aimed to study the effect of changing the perforation number on heat dissipation of the heat sink and investigate if adding more holes would affect positively or negatively on fin performance.

## 2. Theoretical modeling

The heat sink's efficacy is governed by characteristics such as the heat transfer coefficient, Nusselt number, fin performance, and the rate at which heat is transmitted, which is consistent with Newton's second law of cooling:

$$\begin{aligned} Q_{conv} &= h A_s (T_s - T_\infty) \\ &= m_a C_p (T_{out} - T_{in}) \end{aligned} \quad \dots\dots(1)$$

The convective heat transfer rate from the surface of the heat sink to the surrounding air can be determined by using the following equation: -

$$Q_{conv} = Q_{elec} - Q_{loss} \quad \dots\dots(2)$$

Where  $Q_{elec}$  is the electrical heat input and can get its value as follows: -

$$Q_{elec} = IV \quad \dots\dots(3)$$

It can find the average heat transfer coefficient by: -

$$h = \frac{Q_{conv}}{A_s \left( T_s - \frac{T_{out} + T_{in}}{2} \right)} \quad \dots\dots\dots(4)$$

In equation [1], the area  $A_s$  represents the overall surface area of the fin that comes into contact with the fluid flowing through the duct. It is calculated by adding together the projected area and the contribution from the total surface area of the blocks.

Regarding the flat plate fin configuration:

$$A_T = WL + 2N_f H [L+t] + 2B [L+W] \quad \dots\dots\dots(5)$$

In the case of a perforated fin, the area  $A_s$  mentioned in equation [1] encompasses not only the outer surfaces of the fin but also the inner surfaces of the perforations.

$$A_T = WL + 2N_f H [L+t] + 2B [L+W] + N_p N_f d_t - N_p N_f \frac{\pi}{4} d^2 \quad \dots\dots\dots(6)$$

For cross-cut fin:

$$A_T = WL + 2N_f H [L+t] + 2B [L+W] + N_f CH - 2 N_f tH \quad \dots\dots\dots(7)$$

Hence average convection heat transfer coefficient  $h_{av}$  can be finding:

$$h_{av} = \frac{Q_N}{A_T \left[ T_s - \left( \frac{T_{out} + T_{in}}{2} \right) \right]} \quad \dots\dots\dots(8)$$

Now, the thermal resistance is calculated as:

$$R_{th} = \frac{1}{h_{av} A_T} \quad \dots\dots\dots(9)$$

The dimensionless groups are calculated as follows:

The Nusselt number,  $Nu$  is defined as:

$$Nu = \frac{h_{av} D_h}{K_a} \quad \dots\dots\dots(10)$$

In order to more accurately determine the effective velocity at the measurement section within the test section, the average velocity is calculated by:

$$V_{av} = \frac{v}{A - A_{front}} \quad \dots\dots\dots(11)$$

The duct Reynolds number,  $Re$  is defined as:

$$Re = \frac{f a V_{av} D_h}{\mu a} \quad \dots\dots\dots(12)$$

The hydraulic diameter of a rectangular section of the wind tunnel is defined as:

$$D_h = 4 \frac{A_w}{P_w} \quad \dots\dots\dots(13)$$

The bulk mean temperature, which represents the average temperature, is used to obtain the values of thermophysical properties in all calculations:

$$T_m = \frac{T_{out} + T_{in}}{2} \quad \dots\dots\dots(14)$$

The air properties are assessed under normal temperature conditions, known as ambient temperature, denoted as  $T_\infty$ . The heat sink receives heat from the element heater situated on its base. The average temperature of the heat source is  $T_s$ . Once the total thermal resistance value is determined, it becomes possible to calculate the total amount of heat dissipated.

### 3. Experimental Setup

A horizontal forced convection device, is the device that used to accomplish the objective of this study. As cleared in figure [1].

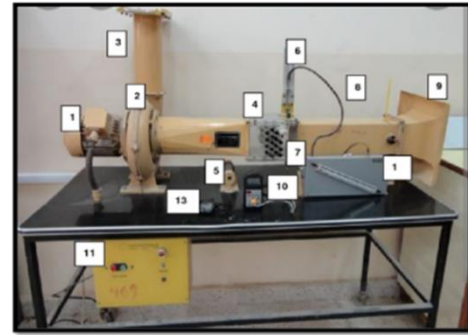


Fig. 1, Forced convection device-horizonal duct.

1-Air blower. 2- Fan. 3- Throttle opening. 4- Test section(which is contain the heat sink). 5- Electrical heater. 6-Total head tube. 7- Test section. 8- Thermometer. 9- Air inlet. 10- Digital thermometer. 11-Control panel. 12- Inclined manometer. 13- Watch the timer.

### 3.1 Experimental Sets

Figure [2] provides a schematic representation of the experimental setup, which encompasses a wind tunnel, a heating system, heat sinks, a blower, and various measurement devices for quantifying temperature and flow velocity. In the wind tunnel system, there is a blower, a test section, and a flow straightener.

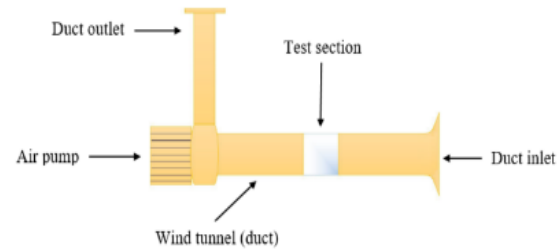


Fig. 2, Schematic diagram of forced convection device.

The heated heat sink effectively dissipates heat to the contacted fluid. The entrance of the duct is designed with a curved shape, resembling a bell mouth, to facilitate the smooth ingress of air into the duct, without the formation of air layers. Positioned at the terminal point of the wind tunnel, a blower with a maximum flow rate of 29.5 m<sup>3</sup>/min extracts the necessary air from the vicinity of the device's surroundings. This air is then expelled through a vertical pipe with a throttle opening diameter of 125 mm. Furthermore, at the exit of the wind tunnel, an adjustable gate is installed to regulate the airflow by selectively opening or closing the pipe, thereby controlling the passage of air through the tunnel. The section of the duct following the test segment includes a flow straightener composed of a honeycomb structure, which promotes the flow of air in a smooth, laminar manner. The horizontal flow duct is constructed from iron with a thickness of 1 mm and has dimensions of a square 125 x 125 mm and a length of 1300 mm. As illustrated in Figure [3], the air flows across the heat sink located within the wind tunnel, facilitating the continuous removal of heat.



**Fig.3 Heat sink inside the test section of the wind tunnel.**

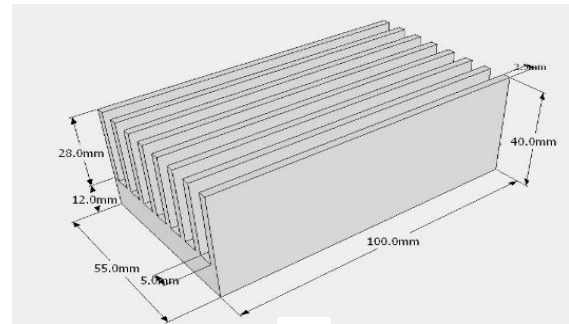
The test section contained all the heat sink samples. These heat sinks are constructed from an aluminum alloy (1006) known for its thermal conductivity of (237) W/m.K. The heat sink base has dimensions of 12 mm (width -  $L_y$ ), 100 mm (length -  $L_x$ ), and 55mm(thickness- $t$ ). This investigation encompasses

three distinct heat sink models, each featuring designs as outlined in Table [1].

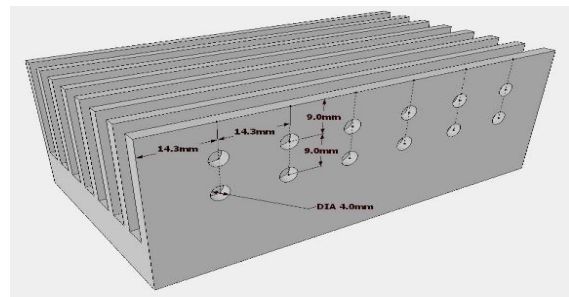
**Table 1 Types of the heat sinks**

Heat sink type	Perforation number (Np)	Surface area (mm <sup>2</sup> )	Weight (gr)
Solid	Non	51420	339.7
PHS-12P	12	52022	307.14
PHS-8P	8	51821	317.7

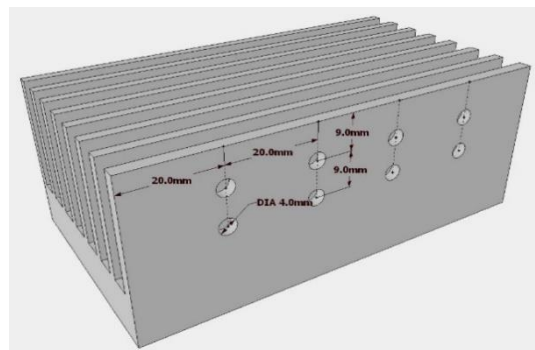
The three samples tested in this paper experimentally are illustrated in figure [4].



**a**



**b**



**c**

**Fig.4, types of heat sinks tested in this study [(a is non-perforated), (b is PHS-12P-perforated heat sink which has 12hole), (c is PHS-8P-perforated heat sink which has 8hole)).**

In order to provide a consistent heat flow surface for heat sinks, an electrical heater-AC- was chosen as a heating source in the system. The airflow rate was used to cool the heated heat sinks at different speeds. A variac-AC- was employed to regulate the power supplied to the heater. This transformer controlled the heating rate by providing a specific voltage to the heater. To ensure complete insulation; the heater body was covered from all sides by Teflon, except for the top where it contacted the heat sink. Three thermocouple holes were positioned at the bottom of the heat sink to measure the required temperatures at the base. The low thermal conductivity of acrylic allowed for neglecting the influence of heat loss from the sides of the test section. Furthermore, surface temperatures were measured at different locations on the acrylic to ensure that heat loss did not significantly affect the results. The findings demonstrated that the temperatures of the acrylic sides were approximately equal to the surrounding temperature due to insulation provided by the heat sink samples. The data acquisition unit consists of a multiplexer, which is employed to capture data from various thermocouples. Anbai AT4516 data logger with a sixteen-channel selector is used to connect the set of thermocouples. K-type thermocouples are utilized to measure the temperature of both the heat sink and the cooling air. All thermocouples used in this study underwent calibration. Three K-type thermocouples were inserted into the heat sink to measure its base temperature. Additionally, eleven thermocouples were affixed to the surface of the heat sink, as shown in Figure [5].

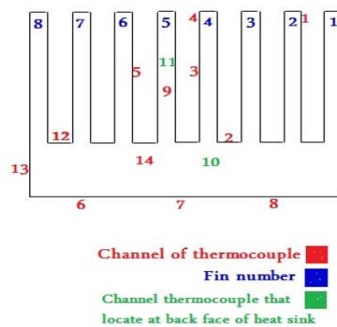


**Fig.5 Thermocouples location on the heat sink.**

The velocity of the airflow entering the wind tunnel's test section was measured using an anemometer from BENETECH, which provided an accuracy of + 5% for velocities ranging from 0 to 30m/s. The evaluation of the heat sink's performance involved

studying both non-perforated and two perforated heat sinks. The non-perforated heat sink, represented by solid rectangular fins without holes (as shown in Figure [4-a]), weighed 339.7 grams. On the other hand, the remaining heat sinks were transversely perforated to enable a comparison between their capabilities in absorbing and dissipating heat from the target objects (as depicted in Figure [4-b and 4-c]). Additionally, all the samples shared the same dimensions, as indicated in Table [2]. They were constructed with a flat plate and extruded rectangular fins measuring 2.5 mm in thickness. The spaces or channels between the fins amounted to 3500 mm<sup>2</sup>, each heat sink featured seven channels with a width of 5 mm. The inclusion of these holes served the purpose of evaluating the heat sink's thermal performance in terms of heat dissipation and cooling rate, while also allowing for a comparison with other samples.

**Table 2. The dimensions of the heat sink.**

Dimensions	Value (mm)
Heat sink width (W)	55
Heat sink length	100
Heat sink base thickness	12
Fin height	28
Fin thickness	2.5
Fin number	8
The interface material thickness	1

### 3.2 Experimental procedures

Once the forced convection device is set up, it is crucial to connect all the necessary components to carry out the experiment effectively. This includes insulating the heating system using a Teflon layer beneath the heater, applying a high thermal conductivity paste between the heater and heat sink, linking the heater to the variac for power control, attaching thermocouples to measure temperature, and fixing an Anemometer to gauge the airflow velocity within the duct via the heat sink. The experimental procedure for each heat sink involves the following steps:



1. Operating the device and select air velocity by opening the gate at outlet pipe until the anemometer read (1.5)m/s.
2. Set the Variac on (20)V, waiting for a period of time until the system stable thermally.
3. Take the readings of temperature at different points on heat sink and at the area of before and after the test section.
4. Increasing the voltage to (40)V and taking readings, then repeat that for (60, 80 and 100)V.
5. Increasing air velocity to (2)m/s and repeat steps (2, 3, and 4). Thus for (2.5, 3, 3.5, 4)m/s.
6. Gathering the experimental readings for all samples to use in calculations. The obtained results analyzed and discussed.

#### 4.Results and discussion

The current paper compared between perforation and non-perforation heat sinks, and between two perforated heat sinks have different perforation numbers. And present this comparison as the effect of that on the thermal performance of fins, and the rate of dissipated heat.

##### a- Changing air velocity:

##### • Heat transfer

The amount of dissipated heat from hot heat sink to the surrounding is an indicator of fin performance. Figure [6] shows the comparison between solid and perforated heat sinks, also shows the effect of perforation number on the rate of heat dissipated(Q). It can be noticed that perforated heat sinks have a higher Q than non-perforated heat sink, where the solid fins read lowest rate of Q, because the perforation adds an extra surface area to the fins for exchanging the heat with contacted air and cooling hot bodies. For perforated heat sinks, PHS-12P has the highest amount of heat dissipated, which improves Q by 6.57%, while the improvements achieved by PHS-8P is 1.75% only at Re 20000. This behavior can be attributed to the number of perforations. Holes enlarge the area of exchanging heat with the air, more holes in the fin means cold air stay for a longer period of time because of the vortex that forms at hole area, and that prolong the heat exchanging between fins and surrounding, resulting in faster cooling process.

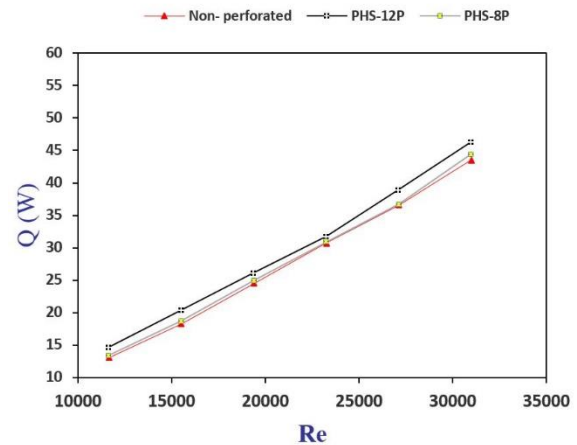


Fig.6 The relation between heat transfer rate versus Reynolds number.

##### • Nusslet number

As Nu is a function of Re, it rises as Re rises. For all types of heat sinks (perforated and non-perforated), Nu has a direct proportion with Re. It is clear from the figure [7] that perforated heat sinks have higher Nu than non-perforated, this is due to the fact that by adding holes, turbulence increased, resulting in improved heat transfer. Furthermore, utilizing a perforated heat sink instead of a solid one enhances the surface area. Specifically, enhance heat dissipation from the heat sink to the surrounding. For perforation effect, as it explained in the figure, the perforation increasing Nu. In the current paper, Nu increase as (22.3%, 8.9%) by two perforated heat sinks (PHS-12P, PHS-8P) respectively at Re 20000. PHS-12P has the highest value of Nu, more holes in the fin cools the heat sink faster.

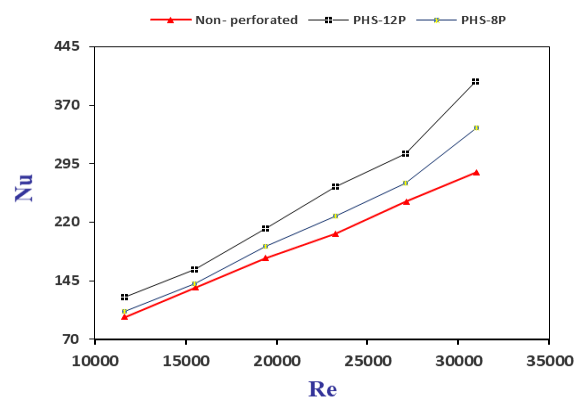


Fig.7 The relation between Nusslet number versus Reynolds number.

### • Fin efficiency $\eta_f$

Figure [8] demonstrates that when Re grows, the efficiency of the fins drops; this figure illustrates that as the perforation number increases, the efficiency of the fin increases. This is as previously stated owing to the bigger surface area offered by more numbers of perforation. Furthermore, the PHS-12P heat sink fins have the most efficiency, with an enhancement ratio of (2.62%), while the PHS-8P has less than the first (an improvement ratio of (0.6%)) at Re30000. In contrast to non-perforated heat sink efficiency.

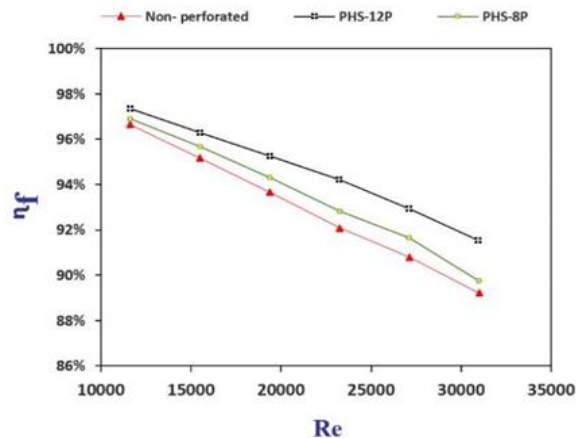


Fig.8 The relation between fin efficiency versus Re

### • Weight reduction

For economic reasons, the mass of the heat sink is critical; lighter heat sinks are preferred. As cleared in Figure [9], increasing the number of perforations reduces the weight of the heat sink. It should be noted that the surface area is inversely proportional to the mass of the heat sink. This behavior indicates that perforating the fins involves removing portions from these fins, which reduces the fins' mass. It can be noticed from the figure that PHS-12P reduced the weight by (9.58%), while PHS-8P reduced by (6.47%) of the solid heat sink's weight.

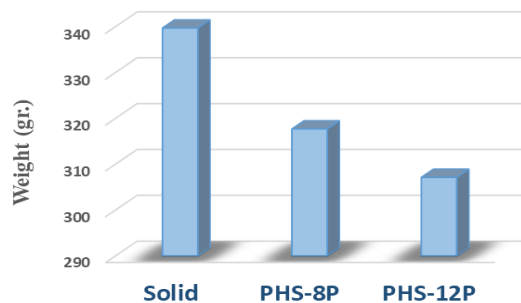


Fig.9 Weight reduction for heat sink

### b-Changing thermal loads:

The results presented previously were at constant voltage (80 v), this section will present the effect of changing the thermal loads (at constant air speed 2.5 m/s) on the thermal performance of heat sink types.

### • Nusslet number and heat transfer coefficient:

As demonstrated in figures [10] and [11], the observed attitude of both Nu and h in the current work is that they increase with increasing thermal loads. When perforated heat sinks PHS-12P and PHS-8P were tested at (80 V), h values increased by (4.93% and 1.52%, respectively). while compared to non-perforated heat sinks, Nu was increased by (1.61%, 4.97%) when utilizing examined heat sinks PHS-8P and PHS-12P, respectively. When testing the PHS-12P, the highest value of h and Nu was obtained, and the minimum value was obtained when testing the non-perforated heat sink. When the thermal load grows, so does the temperature differential between the hot body and its surroundings, resulting in an increase in convective heat transfer coefficient. then raising Nu- because the Nusslet number is the ratio of convective to conductive heat transfer inside a fluid [11].

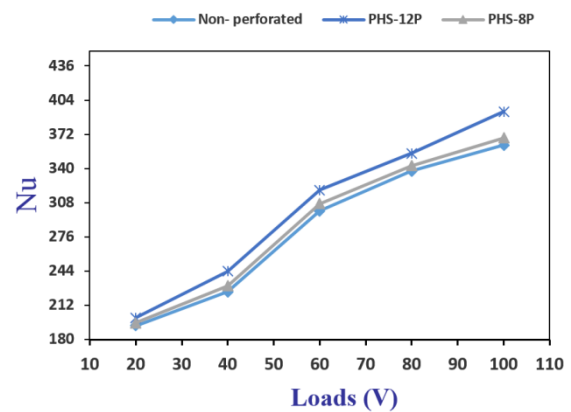
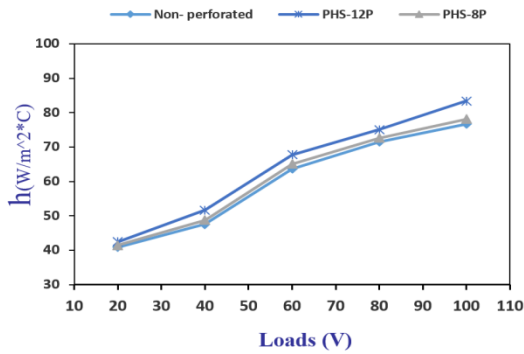


Fig. 10 Variation of Nu with loads



**Fig. 11 Variation of h with loads.**

### • Fin Performance $\eta_f$

Figure [12] shows the fluctuation in fin performance as a result of thermal load impact. As heat loads increase, the performance of the fins decreases. When testing perforated heat sinks (PHS-12P, PHS-8P) at (100V), the fin performance increased by (0.58%, and 0.12%) when compared to non-perforated heat sink. The heat sink (PHS-12P) outperformed the other types in terms of total thermal efficiency. This is because the perforated fin has a larger surface that contacts the surrounding air than the solid fin, resulting in significant heat dissipation.

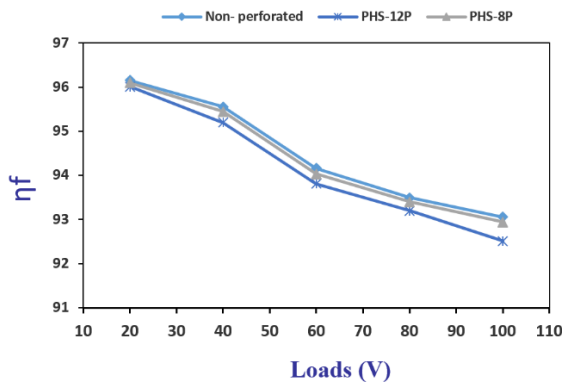


**Fig. 12 Variation of fin performance with loads.**

## 5. Conclusions

A The effect of perforation and perforation number on the thermal performance of the heat sinks has been presented in this paper. PHS-12P and PHS-8P were used and compared with solid heat sink to conclude:

- It is determined that 7.3% of heat is lost through the gaps between heating system layers (between heat

sink and heater, and between the heater and Teflon), also through tunnel walls.

- Increasing the number of perforations (Np) improved heat transfer, as the PHS-8P improved by 1.75%, while the PHS-12P improved by 6.57% when compared to a solid heat sink, implying that perforating four more holes improved heat transfer due to increased surface area by 0.38%.

- When Reynolds number decreases, it concludes that:

- Tout decreases, as a result of low dissipation.
- The temperature difference between heat sink and its surrounding is increases.
- $\eta_f$  increases.
- h decreases, as it is directly proportional with air velocity and surface area. It is noticed that perforation raise the h value by enlarging the heat exchanging area between heat sinks and air flow through the duct.

- The more holes, the greater weight drop, PHS-12P reduced the weight by 9.58% of solid heat sink, while PHS-8P reduce the weight by 6.47% only.

## NOMENCLATURE

Symb ol	Definition	Unit
Q	Heat transfer	W
$h_{av}$	Average heat transfer coefficient	$W/m^2.K$
T	Temperature	$^{\circ}C$
$T_s$	Surface temperature	$^{\circ}C$
$T_{\infty}$	Mean temperature	$^{\circ}C$
$T_{in}$	Temperature at inlet area	$^{\circ}C$
$T_{out}$	Temperature at outlet area	$^{\circ}C$
$T_m$	Mean temperature	$^{\circ}C$
$\Delta T$	Temperature difference	$^{\circ}C$
W	Duct cross section width	mm
A	Area	$mm^2$
$A_c$	Cross sectional area	$mm^2$
$A_s$	Surface area	$mm^2$
$A_{sf}$	Surface area of fin	$mm^2$
$A_{ss}$	Surface area of fin space	$mm^2$



$A_p$	Perforation area	$\text{mm}^2$
$N_p$	Perforation number	-
$N_f$	Fins number	-
$W_f$	Fin width(fin thickness)	mm
$L_f$	Fin length	mm
$H_f$	Fin height	mm
$\dot{Q}_{\text{conv}}$	Convective heat transfer	W
$\dot{Q}_{\text{cond}}$	Conductive heat transfer	W
$\dot{Q}_{\text{rad}}$	Radiative heat transfer	W
$\dot{Q}_{\text{elect}}$	Electric heat transfer	W
$I$	Current	A
$V$	Voltage	V
$v$	Air velocity	m/s
$K$	Thermal conductivity	W/m.K
$Re$	Reynolds number	-
$Nu$	Nusslet number	-
$m$	Mass	Kg
$\dot{m}$	Mass flow rate	kg/s
$C_p$	Specific heat at constant pressure	J/kg.K
$P_p$	Perforation perimeter	mm
$D_p$	Perforation diameter	mm
$P_s$	Perforation space	-
$A_h$	Hole area	$\text{mm}^2$
$N_s$	Space number	-
$R$	Thermal resistance	$^{\circ}\text{C}/\text{W}$
$R_{\text{conv}}$	Convective resistance	$^{\circ}\text{C}/\text{W}$
$R_{\text{cond}}$	Conductive resistance	$^{\circ}\text{C}/\text{W}$
$d_h$	Hydraulic diameter	mm
$A_d$	Cross-sectional area of duct	$\text{mm}^2$
$P_d$	Perimeter of duct	mm

#### Greek Symbols

Symbol	Definition	Unit
$\emptyset$	Hole diameter (perforation)	-
$\nu$	Kinematic viscosity	$\text{m}^2/\text{s}$

$\rho_{\text{air}}$	Density of air	$\text{Kg}/\text{m}^3$
$\eta$	Thermal efficiency	-
$\varepsilon_f$	Fin effectiveness	-
$\Theta_b$	Temperature difference	-

#### Subscripts

Symbol	Definition
Av	Average
Base	Heat sink base
Fin, Fins	Heat sink fin
In	Inlet
Out	Outlet
M	Mean
$\infty$	Infinity
Re	Reynolds number
Nu	Nusslet number
Pr	Prandtle number

#### References

- [1] Sakkarin Ch. a,b, Somchai W., “A review of the effect of flow directions and behaviours on the thermal performance of conventional heat sinks”, International Journal of Heat and Mass Transfer, 81 (2015) 10–18.
- [2] Jin-Cherng Sh., Jhao-Siang J., “Heat Transfer Enhancement of Plate-Fin Heat Sinks with Different Types of Winglet Vortex Generators”, Energies, 2020, 13, 5219.
- [3] Wei Wang<sup>1,2</sup> · Yongji Li<sup>1</sup> · Yaning Zhang<sup>1</sup> · Bingxi, “Analysis of laminar flow and heat transfer in an interrupted microchannel heat sink with different shaped ribs”, Journal of Thermal Analysis and Calorimetry, 10973-019.
- [4] Qifeng Zhu , Yangyang Jin , Junjie Chen, “Computational study of rib shape and configuration for heat transfer and fluid flow characteristics of microchannel heat sinks with fan-shaped cavities”, Applied Thermal Engineering, 195 (2021) 117171.
- [5] Kim O.N. ,Sara, T. Pekdemir, S. Yapici, M. Yilmaz, “Heat-transfer enhancement in a channel flow with perforated rectangular blocks”, J heat and fluid flow,22 (2001) 509-518.
- [6] M.R. Shaeri, M. Yaghoubi, K. Jafarpur, “Heat transfer analysis of lateral perforated fin heat sinks”. Applied Energy, 86 (2009) 2019–2029.
- [7] Venkitaraj K.P., sanoj Kidikh, “Natural Convection Heat Transfer Enhancement from Rectangular Fin Arrays with Divers Geometrical Perforations” 2016, 78-1-4673-9925-8.

- [8] Rahul S., D.D. Palande, "Heat Transfer Enhancement by using perforation: A Review", IRJET, (2016) 2395-0072.
- [9] Mohammed R. Shaeri, R. Bonner, "Laminar forced convection heat transfers from laterally perforated-finned heat sinks", App. Thermal Engineering 2017 (116) 406–418.
- [10] Sakkarin C., Ho Seon, Lazarus G.A., Smochai W., "Fluid flow and heat transfer characteristics of heat sinks with laterally perforated plate fins", International Journal of Heat and Mass Transfer, 138 (2019) 293–303.
- [11] Cheng-Hung Huang, Yaun-Rei Huang, "An optimum design problem in estimating the shape of perforated pins and splitters in a plate-pin-fin heat sink", International Journal of Thermal Science, 170 (2021) 107096.759,2018.